doi:10.1006/jmbi.2001.4588 available online at http://www.idealibrary.com on IDEAL® *J. Mol. Biol.* (2001) **309**, 423–435

JMB

# Conformational Changes in *Leishmania mexicana* Glyceraldehyde-3-phosphate Dehydrogenase Induced by Designed Inhibitors

**Stephen Suresh[1,2], Jerome C. Bressi[3], Kevin J. Kennedy[3] Christophe L. M. J. Verlinde[1], Michael H. Gelb[3,4] and Wim G. J. Hol[1,2,4]***

[1]*Departments of Biological Structure, Biomolecular Structure Center*

[2]*Howard Hughes Medical Institute*

[3]*Department of Chemistry*

[4]*Department of Biochemistry University of Washington Seattle, WA 98195, USA*

**Corresponding author*

The glycolytic enzymes of trypanosomes are attractive drug targets, since the blood-stream form of *Trypanosoma brucei* lacks a functional citric acid cycle and is dependent solely on glycolysis for its energy requirements. Glyceraldehyde-3-phosphate dehydrogenases (GAPDH) from the pathogenic trypanosomatids *T. brucei*, *Trypanosoma cruzi* and *Leishmania mexicana* are quite similar to each other, and yet have sufficient structural differences compared to the human enzyme to enable the structure-based design of compounds that selectively inhibit all three trypanosomatid enzymes but not the human homologue.

Adenosine analogs with substitutions on N-6 of the adenine ring and on the 2′ position of the ribose moiety were designed, synthesized and tested for inhibition. Two crystal structures of *L. mexicana* glyceraldehyde-3-phosphate dehydrogenase in complex with high-affinity inhibitors that also block parasite growth were solved at a resolution of 2.6 Å and 3.0 Å. The complexes crystallized in the same crystal form, with one and a half tetramers in the crystallographic asymmetric unit. There is clear electron density for the inhibitor in all six copies of the binding site in each of the two structures. The *L. mexicana* GAPDH subunit exhibits substantial structural plasticity upon binding the inhibitor. Movements of the protein backbone, in response to inhibitor binding, enlarge a cavity at the binding site to accommodate the inhibitor in a classic example of induced fit. The extensive hydrophobic interactions between the protein and the two substituents on the adenine scaffold of the inhibitor provide a plausible explanation for the high affinity of these inhibitors for trypanosomatid GAPDHs.



*Keywords:* GAPDH; trypanosomatids; drug design; inhibitors; X-ray structure

## Introduction

Trypanosomatids are protozoa that cause many severe global diseases affecting both people and livestock.[1,2] *Trypanosoma brucei* subspecies cause African sleeping sickness in humans and nagana in sheep and cattle. *Trypanosoma cruzi* causes Chagas' disease in Latin America, and various *Leishmania* species cause a number of diseases collectively called leishmaniasis, occurring throughout the tropics. Despite the highly destructive nature of these diseases and the large number of people affected by them, no good therapy exists. The drugs presently in use are unsatisfactory, since many cannot

Abbreviations used: GAPDH, glyceraldehyde-3-phosphate dehydrogenase; TNDBA, $N^6$-(1,2,3,4-tetrahydronaphthyl)-2′-deoxy-2′-(3,5-dimethoxy benzamido)adenosine; NMDBA, $N^6$-(1-naphthalene methyl)-2′-deoxy-2′-(3,5-dimethoxy benzamido)adenosine; DMSO, dimethyl sulfoxide; PMSF, phenylmethylsulfonyl fluoride; WHO, World Health Organization.

E-mail address of the corresponding author: hol@gouda.bmsc.washington.edu

0022-2836/01/0000423–13 $35.00/0

be given orally and they are hampered by severe toxicity and increasing resistance of the parasites.[3] For example melarsoprol, the only drug against late-stage *T. brucei rhodesiense* infections, is so poisonous that 5-10 % of the patients die because of toxic side-effects.[4] Thus, there is an urgent need for more effective and safer drugs.

The distinctive metabolic pathways of these parasites, in particular their major dependence on glycolysis for energy, suggests that the glycolytic enzymes would be viable targets for chemotherapy.[4,5] For example, the blood-stream form of *T. brucei* that lives in the human host is entirely dependent on glycolysis for ATP production as it lacks a functional tricarboxylic acid cycle.[6] These organisms have a specialized organelle called the glycosome, where the first seven enzymes involved in glycolysis are sequestered, and within which glycolysis proceeds at a very high rate.[7] Inhibiting these enzymes of the glycolytic pathway would therefore be a promising way to block parasite growth. It has been shown that blocking glucose metabolism in *T. brucei* parasites in infected mammalian hosts kills the parasites, lending validity to the role of glycolytic enzymes as trypanosomal drug targets.[8] We have targeted the following glycosomal enzymes for structure-based drug design: triose phosphate isomerase,[9,10] phosphoglycerate kinase,[11,12] aldolase,[13] glycerol-3-phosphate dehydrogenase[14] and glyceraldehyde-3-phosphate dehydrogenase (GAPDH).[15–18] Trypanosomal triose phosphate isomerase and GAPDH have been pursued as drug targets by other groups as well.[19,20] Computer modeling of the metabolic pathway in the glycosomes of trypanosomes[21] indicates that GAPDH exerts considerable control on the glycolytic flux. Therefore, inhibiting GAPDH appears to be a promising way to curb glycolysis in these parasites.

GAPDH is a homotetramer with D2 symmetry and molecular mass 156 kDa that catalyses the oxidative phosphorylation of glyceraldehyde-3-phosphate to 1,3-bis-phosphoglycerate using $NAD^+$ as a cofactor. Based on the structures of *T. brucei* and *L. mexicana* GAPDH complexed with $NAD^+$ determined in our laboratory,[15,17] a number of adenosine-based inhibitors were designed, synthesized and tested against GAPDH from *Leishmania mexicana*, *T. brucei*, *T. cruzi* and *H. sapiens*.[22,23] Several disubstituted adenosine derivatives were demonstrated to be potent selective inhibitors of the three trypanosomatid enzymes but not of the human enzyme.[24] Some of these disubstituted compounds have even shown promise in inhibiting the growth of cultured blood-stream *T. brucei* and intracellular *T. cruzi*.[18] Here, we present the crystal structures of *L. mexicana* GAPDH in complex with two of these selective high-affinity inhibitors, namely $N^6$-(1-naphthalenemethyl)-2′-deoxy-2′-(3,5-dimethoxybenzamido)adenosine (NMDBA), and $N^6$-(1,2,3,4-tetrahydronaphthyl)-2′-deoxy-2′-(3,5-dimethoxybenzamido)adenosine (TNDBA). Interesting and unexpected changes in the GAPDH structure are observed and will be discussed.

## Adenosine derivatives as selective GAPDH inhibitors

Active sites of enzymes are often highly conserved across species, making it difficult to design selective compounds that inhibit the parasite enzyme but not the human homologue. In favorable cases, when the parasite enzyme utilizes a sizeable cofactor, it is possible to circumvent this obstacle, since there are usually significant structural differences in regions of the protein that bind parts of the cofactor distant from the ''core'' of the active site. Such differences offer opportunities for the design of selective inhibitors. This is the case with GAPDH, where the human enzyme shares a sequence identity of 50-53 % with the trypanosomatid homologues. Parts of the enzyme at the active site near the nicotinamide end of the cofactor binding site are highly conserved between humans and the three trypanosomatids *L. mexicana*, *T. brucei* and *T. cruzi*.[15,17,20,25] In contrast, further away from the active site, near the adenosine binding region, many significant structural differences occur between the human GAPDH and the three trypanosomatid enzymes.[22]

Analysis of the pocket on GAPDH that binds the adenosyl portion of $NAD^+$ furnished us with four regions where differences between the trypanosomatid and human GAPDHs occur, that could be exploited for the design of selective inhibitors.[22] Close to the C-2 atom of the adenine ring, *L. mexicana* GAPDH has a hydrophobic residue (Val37), instead of the hydrophilic Asn33 in the human enzyme (Figure 1). Modeling studies indicated that a methyl substitution at C-2 could be accommodated by a small pocket that is present in the trypanosomatid enzyme but is less pronounced in the human enzyme. Another region of interest is located near N-7 and C-8 of adenine. In *L. mexicana* GAPDH, Leu113 comes closer to the adenine ring than the equivalent Val100 of the human enzyme. Hydrophobic substituents that pack against Leu113 could therefore gain affinity as well as selectivity. A third region where substituents on the adenosine scaffold were considered is at the N-6 position of the adenine ring. In *L. mexicana* GAPDH this region is quite hydrophobic, since it is formed by Met39, Leu113, Phe114 and the side-chain methylene units of Arg92. The N-6 amino group itself makes a hydrogen bond with the backbone carbonyl group of Gln91, which was sought to be preserved in the design of $N^6$ substituents. The fourth region that was exploited for the design of potent selective inhibitors is near O-2′ of the adenosine ribose. In *L. mexicana* GAPDH there is a mostly hydrophobic cleft near O-2′, composed of Met39 on one side and Val206* from a neighboring monomer on the other. In the human enzyme there is no such cleft, since the protein backbone traces a different path, bringing Phe36 and Ile37 from one

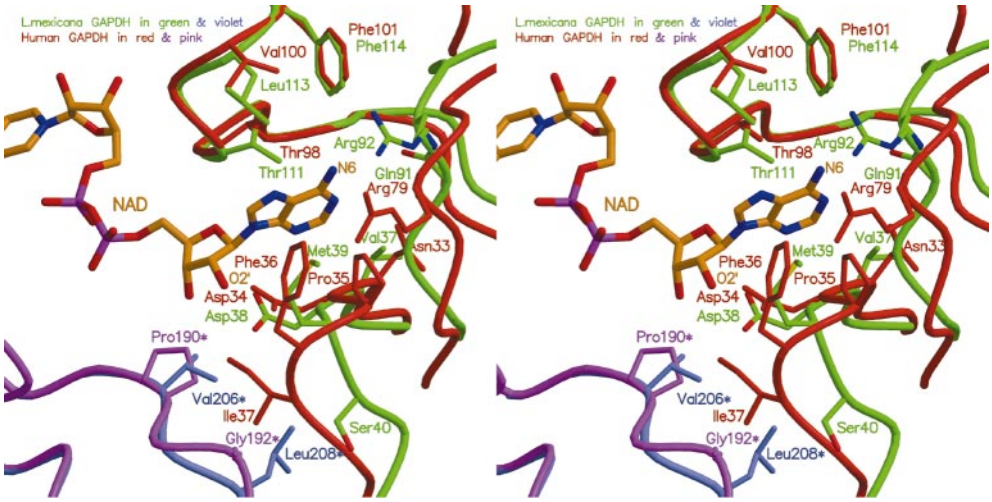


**Figure 1.** Superposition of *L. mexicana* GAPDH (green and violet) and human GAPDH (red and pink), highlighting differences in the region of the protein binding the adenosine part of the $NAD^+$ cofactor.[17,25] The bound $NAD^+$ from the *L. mexicana* GAPDH structure is shown in gold. Of particular relevance to our drug design efforts is the cleft in *L. mexicana* GAPDH, between Met39 of one monomer (green) and Val206* of the neighboring monomer (violet, marked with a *). In the human enzyme this selectivity cleft is absent, since the protein backbone in this region (Pro35 to Ile37 in red) traces a different path and is therefore much closer to Pro190* of the neighboring monomer (pink). In this and other Figures, only the main-chain atoms of Gln91 have been shown, since it is the main-chain carbonyl group that makes a hydrogen bond to N-6 of the adenine residue. This Figure was made with MOLSCRIPT[38] and rendered with Raster3D.[39,40]

monomer, close to Pro190* from the neighboring monomer (Figure 1). Adenosine derivatives with substituents at the O-2′ position that fill this ''selectivity cleft'' of the trypanosomatid GAPDHs were predicted to have substantial gains in selectivity as well as affinity. Since the 2′-hydroxyl group makes an important hydrogen bond to the conserved Asp38, it was thought necessary to preserve this hydrogen bond while designing derivatives. This was achieved by the replacement of the 2′-hydroxyl group by an amino group that could be derivatized to an amide group with suitable hydrogen bond properties.

The first cycle of design and synthesis of adenosine derivatives produced a number of inhibitors with improved binding to, and increased selectivity for, the trypanosomatid GAPDHs.[22] The addition of a methyl group at the C-2 position of adenosine, improved the $IC_{50}$ to 6 mM against *L. mexicana* GAPDH, an eightfold enhancement over adenosine, which has an $IC_{50}$ of 50 mM. A benzyl substitution at the N-6 position resulted in tenfold tighter binding than adenosine, while a naphthalene methyl group at N-6 generated a molecule with an $IC_{50}$ of 150 μM, an improvement of 330-fold over adenosine. A thienyl group at the C-8 position of adenosine was also promising, with 100-fold improvement in binding. Inhibitors with groups that could occupy the ''selectivity cleft'' of the trypanosomatid GAPDHs were created through an amido linkage to the 2′ position of 2′-deoxy adenosine. These 2′ derivatives of adenosine were very selective trypanosomatid inhibitors. For example 2′-deoxy-2′-(3-methoxybenzamido) adenosine inhibited *L. mexicana* GAPDH with an $IC_{50}$ of 0.3 mM, but had a $IC_{50}$ of >10 mM against the human enzyme, a selectivity of more than 33-fold.

In contrast to the differences between the human and the three trypanosomatid enzymes, the adenosine binding environment is quite conserved among the trypanosomatids. *L. mexicana* GAPDH therefore serves as a valid model of the *T. brucei* and *T. cruzi* enzymes as well, sharing a sequence identity of 81% and 85% with each of them, respectively. In particular, at the adenosine binding region the sequences and structures are virtually identical, with the sole exception of Ser40 in *L. mexicana* GAPDH, where the equivalent residue is asparagine in the other two trypanosomatid enzymes. Therefore, inhibitors designed utilizing the *L. mexicana* structure might be effective against the *T. brucei* and *T. cruzi* enzymes as well, enabling us to target the enzymes from all three parasites simultaneously.

## Additivity and non-additivity of multiple substituents on adenosine

After the design, synthesis and testing of a number of monosubstituted adenosine derivatives, the possibility of increased affinity and improved selectivity of disubstituted compounds with modifications on both the adenine ring and the 2′ position on the ribose was explored.[23] It was found that substitutions either on the C-2 or the C-8 position of adenine were sterically incompatible with substitutions at the 2′ position, leading to decreased affinity of these disubstituted compounds compared to the corresponding monosubstituted adenosine derivatives. On the other hand,

substitutions at the N-6 position that improved affinity could be coupled with substitutions at the 2′ position that occupied the selectivity cleft, producing a series of compounds with dramatically enhanced affinity and selectivity.[18] The disubstituted adenosine derivative, $N^6$-(1,2,3,4-tetrahydronaphthyl)-2′-deoxy-2′-(3,5-dimethoxy benzamido) adenosine (TNDBA) inhibits *L. mexicana* GAPDH with an $IC_{50}$ of 75 μM, while $N^6$-(1-naphthalene methyl)-2′-deoxy-2′-(3,5-dimethoxy benzamido) adenosine (or NMDBA) has an $IC_{50}$ of 2 μM (J. C. Bressi *et al.*, personal communication), an improvement of over four orders of magnitude over adenosine. As a prelude to the design and synthesis of the next cycle of inhibitors, we have determined the crystal structure of *L. mexicana* GAPDH in complex with these two potent inhibitors, NMDBA and TNDBA.

## Results and Discussion

### Crystal structure of *L. mexicana* GAPDH in complex with NMDBA and TNDBA

The crystal structure of *L. mexicana* GAPDH in complex with NMDBA was determined to a resolution of 2.6 Å (see Materials and Methods). The crystals belong to space group $P2_12_12$ (Table 1) and contain one tetramer in a general position (chains A, B, C and D) and another tetramer positioned with an intramolecular 2-fold coincident with the crystallographic 2-fold (chains E and F and their crystallographic symmetry equivalents). The asymmetric unit therefore contains one and a half GAPDH tetramers with a total of 233 kDa per asymmetric unit. The six monomers in the asymmetric unit were refined using CNS[26] with non-crystallographic symmetry restraints to an *R*-factor of 20.5 % and an $R_{free}$ of 25.6 % (for 5 % of the reflections). The six monomers are very similar and superpose among themselves with rmsd values between 0.12 Å and 0.25 Å for 358 $C^{\alpha}$ atoms, although the average temperature factors of the different monomers vary between 40 $Å^2$ for chain C and 58 $Å^2$ for chain F. The structure is well determined with 88.1 % of the residues in the most favored regions of the Ramachandran map and, with one exception, the rest of the residues are in the additionally allowed regions (10.9 %) and generously allowed regions (0.7 %). The single residue (Val255) in the disallowed region of the Ramachandran map is a general structural feature of the GAPDHs, since it is conserved among *T. brucei*, human, *Bacillus stearothermophilus*, lobster and *Escherichia coli* proteins,[15,27–29] and in all these structures it is in the same region of the Ramachandran map, with ($\phi$,$\psi$) values around (88°,131°). After refining the protein model, $F_o - F_c$ and $2F_o - F_c$ maps were calculated, that revealed clear density for the inhibitor in all six independent binding sites in the crystal structure. Sixfold non-crystallographic symmetry averaging further improved the electron density (Figure 2(a)), unequivocally establishing the binding mode of NMBDA.

**Table 1.** Data collection and refinement statistics

| | NMDBA | TNDBA |
|---|---|---|
| Space group | $P2_12_12$ | $P2_12_12_1$ |
| Cell parameters (Å) | $a = 80.4$, $b = 394.1$, $c = 71.90$ | $a = 80.5$, $b = 393.6$, $c = 70.4$ |
| Resolution (Å) | 2.6 | 3.0 |
| Observations | 407,373 | 179,302 |
| Unique reflections | 65,878 | 44,685 |
| Completeness (%)[a] | 94.0 (71.7) | 96.4 (89.6) |
| $R^a_{merge}$ | 0.066 (0.289) | 0.068 (0.200) |
| $I/\sigma_I$ | 29.3 (4.7) | 23.1 (5.6) |
| Refinement | | |
| rmsd from ideality | | |
| Bond lengths (Å) | 0.007 | 0.009 |
| Bond angles (deg.) | 1.28 | 1.30 |
| $R^a_{cryst}$ | 0.205 (0.299) | 0.211 (0.327) |
| $R^a_{free}$ (5 % of reflections) | 0.256 (0.368) | 0.267 (0.376) |
| Number of atoms | | |
| Protein | 16,296 | 16,296 |
| Waters | 657 | 0 |
| Inhibitor | 252 | 246 |
| Average *B*-factors ($Å^2$) | | |
| Main-chain | 45.2 | 43.7 |
| Side-chain | 49.1 | 47.3 |
| Water | 38.7 | - |
| Inhibitor | 67.5 | 66.5 |

[a] Values in parentheses refer to outermost shell.

The crystals of *L. mexicana* GAPDH in complex with TNDBA grew in the same space group, with cell parameters similar to those of the complex with NMDBA, and diffracted to 3 Å (Table 1). The protein model from the NMDBA structure (after omitting the inhibitor) was therefore used as the starting point for the refinement of the TNDBA complex. After simulated annealing with CNS,[26] 6-fold non-crystallographic symmetry averaging was performed. The averaged map (prior to modeling in TNDBA), had clear density for all six copies of TNDBA in the structure (Figure 2(b)). The complexes of *L. mexicana* GAPDH with NMDBA and TNDBA are very similar, and the complete tetramers in the asymmetric units of these two structures superpose with an rmsd of 0.2 Å. The inhibitors adopt the essentially same binding mode, as can be seen from Figure 2(d). As the complex with NMDBA has the higher resolution of 2.6 Å, this complex was used primarily in the analysis of the structure.

### Interactions of inhibitor with the protein

The inhibitor NMDBA binds in a similar fashion in the six copies of the GAPDH monomer in the asymmetric unit (Figure 2(c)). Consistent with the variability in the average temperature factors of the protein atoms in the different monomers, the mean temperature factors of NMDBA atoms vary from 49 $Å^2$ for chain C to 83 $Å^2$ for chain F. Since chain C is the most ordered, as reflected by its low temperature factors, it was used as the reference

molecule in the analysis. NMDBA makes a large number of close interactions with its target enzyme, with parts of it inserting into the selectivity cleft between adjacent monomers.

The benzamido group of NMDBA[18,22] inserts into the selectivity pocket of *L. mexicana* GAPDH, packing against $C^{\beta}$ and $C^{\gamma}$ of Met39 on one side and Val206* from a symmetry-related protein molecule on the other (Figures 2(c) and 3(a)). The methoxy group closest to the ribose inserts into a cavity of the protein, with the methyl group making a hydrophobic interaction with Phe46 that lines this cavity. The other methoxy group on the benzamido group is largely solvent-exposed, although its methyl group makes a hydrophobic interaction with Leu208* from the neighboring monomer. As in the holo enzyme structure, the 3′-hydroxyl group on the ribose makes a hydrogen bond to $O^{\delta 2}$ of the conserved Asp38. Also, the -NH of the amido group linking the benzamido group to the ribose makes a hydrogen bond with $O^{\delta 1}$ of Asp38. The binding mode is similar in the six copies of the inhibitor in the asymmetric unit (Figure 2(c)), with the length of this hydrogen bond varying between 2.9 Å and 3.4 Å. Thus the hydrogen bond between the 2′-hydroxyl group of the adenosine ribose and this aspartate in the holo complex is preserved by the use of the amido group to link the dimethoxy benzene to the ribose, exactly as predicted.[22]

As in the holo complex, the adenine ring occupies the cavity between Met39 on one side and Thr111 and Leu113 on the other. The five-membered ring of adenine makes hydrophobic interactions with $S^{\delta}$ and $C^{\varepsilon}$ of Met39, while the six-membered ring of adenine packs against $C^{\beta}$ of Ala90 and $C^{\gamma}$ of Thr111. In all six copies in the asymmetric unit, N-1 of adenine makes a hydrogen bond to an ordered water molecule. As in the holo complex, the nitrogen atom at the six position of adenine (N-6) makes a hydrogen bond to the main-chain carbonyl group of Gln91. The length of this hydrogen bond varies from 2.9-3.3 Å in the six independent subunits in the crystal structure.

The naphthylene methyl substitution at the N-6 position of adenine interacts with $S^{\delta}$ and $C^{\varepsilon}$ of Met39 on one side and the hydrophobic part of the side-chain of Arg92 on the other. The atoms of the guanidyl side-chain of Arg92 have high temperature factors, indicative of flexibility of this surface residue. The second ring of the naphthyl group is partially solvent-exposed and comes close to Leu113. The previously noted[18] higher affinity of the naphthylene methyl group at the N-6 position, as compared to the benzyl group, could be possibly due to transient favorable interactions that the second ring of the naphthyl group makes with the flexible side-chain of Arg92 and the hydrophobic side-chain of Leu113.

The difference between the inhibitors NMDBA and TNDBA is the substitution at the N-6 position of the adenine scaffold. In NMDBA the naphthyl group is connected to N-6 by a methylene linkage. In contrast in TNDBA, the methylene linkage is absent and one of the naphthylene rings is saturated. The two-ringed substituent in TNDBA (Figure 2d and Figure 3(b)) is therefore closer to N-6, as compared to NMDBA, and the saturated ring is non-planar, as opposed to the planar naphthyl moiety of NMDBA. As a consequence of being closer to N-6, the saturated ring of TNDBA makes a hydrophobic interaction with the side-chain atoms of Leu113. The second (aromatic) ring of TNDBA occupies approximately the same position as the first ring of the naphthyl moiety in NMDBA (Figure 2(d)), packing between the side-chain atoms of Met39 and Arg92. Of the two possible predicted binding modes for substituents at N-6,[24] the substituents in both complexes adopt the same binding mode in all six copies in the asymmetric unit. The two structures, therefore confirm the predicted binding mode[24] of these hydrophobic substituents at N-6, and are consistent with the low-resolution (3.5 Å) structure of *L. mexicana* GAPDH with $N^6$-benzyl NAD, previously determined in our laboratory.[18]

The dimethoxybenzamido and the methylnaphthyl substituents of NMDBA were both designed to fit hydrophobic cavities extending from the 2′ and N-6 positions of adenine, respectively. The binding mode is fully confirmed by the structure of our binary enzyme:inhibitor complex. The two substituents wrap around Met39, which is conserved among the trypanosomatids. The tight binding of this disubstituted adenosine analogue (NMDBA) is exemplified by the extensive interaction that it makes with the protein molecule, as reflected in the large solvent-accessible surface area that is buried upon forming the complex. The dimethoxy benzamido group buries approximately 368 $Å^2$ of accessible surface area on binding *L. mexicana* GAPDH in each of the six monomers in the asymmetric unit, while the naphthylene methyl group buries about 332 $Å^2$. In comparison, the adenosine scaffold buries about 530 $Å^2$ of accessible surface area on the enzyme. Therefore, out of a total buried accessible surface upon NMDBA binding of 998 $Å^2$, the two substituents dimethoxybenzamido and methylnaphthyl together bury a total of 700 $Å^2$, considerably more than the 530 $Å^2$ buried by the adenosine scaffold though parts of the area buried by the substituents overlaps with the area buried by adenosine.

## Structural changes upon inhibitor binding

The structures of *L. mexicana* GAPDH in complex with $NAD^+$ and in complex with the selective inhibitor NMDBA are similar, and the tetramers superpose with an rmsd of 0.99 Å. Despite the overall similarity of the two structures, parts of the protein backbone move by as much as 2.5 Å. The majority of the movements are in the N-terminal $NAD^+$-binding domain (residues 1-169), parts of which exhibit considerable plasticity upon binding the disubstituted adenosine analogue, although the entire N-terminal domains from the $NAD^+$ and

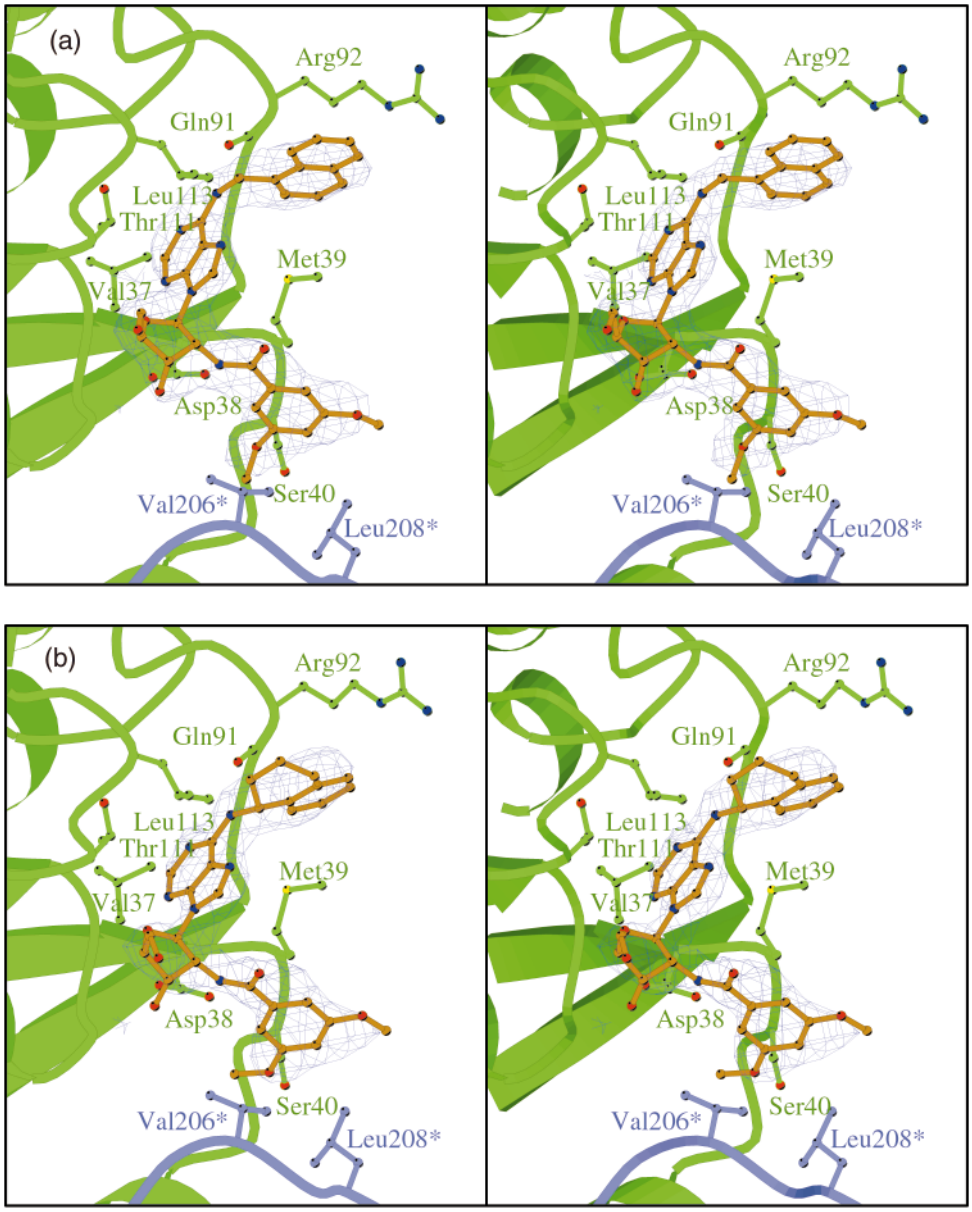


**Figure 2** (*legend opposite*)

NMDBA complexes superpose with rmsd values of approximately 0.7 Å. The C-terminal substrate-binding domain (residues 170-358) is largely unchanged, with the exception of the polypeptide segment between Thr225 and Gly245, with the entire C-terminal domains superpose with rmsd values of approximately 0.4 Å.

Among the structural changes in the $NAD^+$-binding domain, of particular interest are the large displacements at the inhibitor binding site. As mentioned earlier, the dimethoxybenzamido group inserts itself into the so-called selectivity cleft between Met39 of one monomer and Val206* of a neighboring monomer. In the inhibitor complex, the portion of the polypeptide (residues 35-42) around Met39, moves away from Val206* enlarging the cleft (Figure 4). In the holo enzyme complex of *L. mexicana* GAPDH with $NAD^+$,[17] the shortest distance between the side-chain atoms of Met39 ($C^{\beta}$) and Val206* ($C^{\gamma 1}$ from a neighboring monomer) that delineate the two sides of this pocket, ranges between 4.6 and 5.2 Å in the four copies in the asymmetric unit. In the inhibitor complex (with the dimethoxybenzamido group inserted into this pocket) the distance is considerably larger and varies between 7.2 and 7.6 Å. The selectivity cleft thus expands by more than 2 Å upon binding of the inhibitor to permit the insertion of the benzamido group into the cleft in an example of classic induced fit. Despite the fact that the dimethoxy-

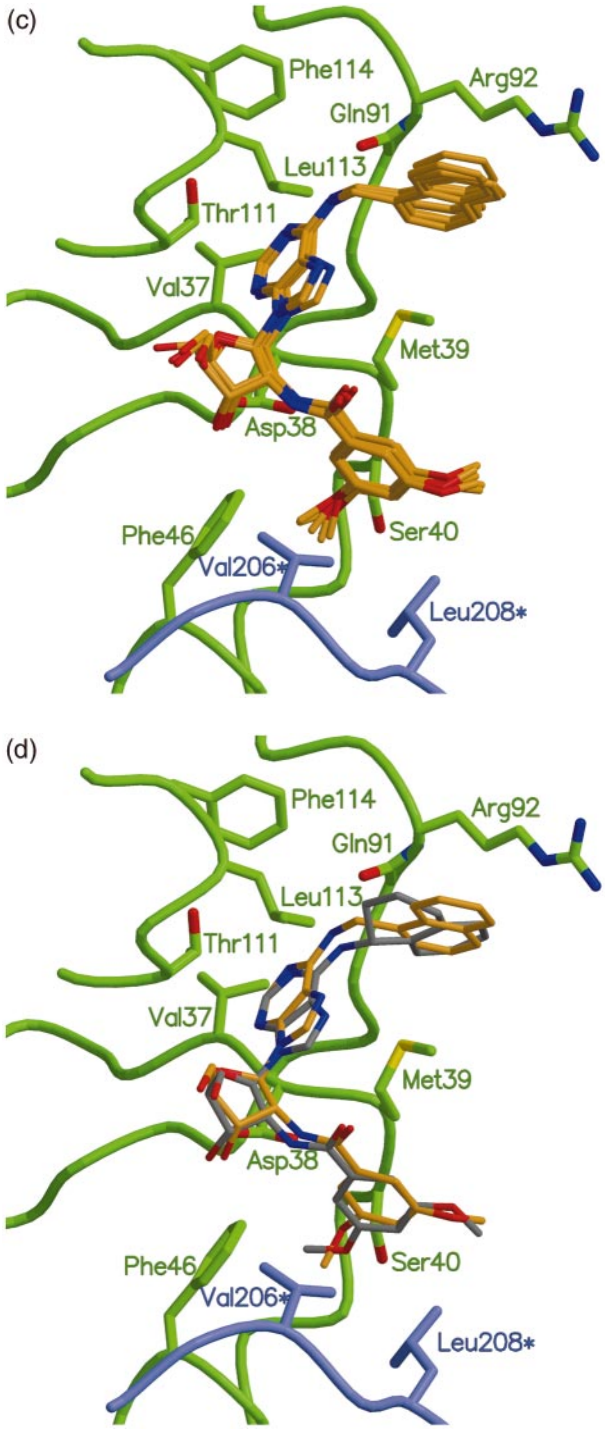


**Figure 2.** (a) Model-unbiased 6-fold averaged $2F_o - F_c$ map of NMDBA bound to *L. mexicana* GAPDH at 2.6 Å contoured at 0.82σ to within 2.0 Å of NMDBA atoms. The map was calculated after refining the six protein monomers in the asymmetric unit and prior to modeling in the bound inhibitor (NMDBA, gold C atoms). In (a)-(d) residues in green and violet are from adjacent monomers of the biological tetramer. (b) Model-unbiased sixfold averaged $2F_o - F_c$ map of TNDBA bound to *L. mexicana* GAPDH at 3.0 Å, contoured at 0.82σ to within 2.0 Å of TNDBA atoms. (a) and (b) were made with Bobscript.[41] (c) Superposition of the six copies of the bound inhibitor NMDBA (gold C atoms), in the crystal structure in complex with *L. mexicana* GAPDH. The 358 $C^{\alpha}$ atoms of each monomer were used in the superposition. (d) Superposition of the crystal structures of *L. mexicana* GAPDH in complex with NMDBA (gold) and the structure in complex with TNDBA (grey). (c) and (d) Created with MOLSCRIPT[38] and Raster3D.[39,40]

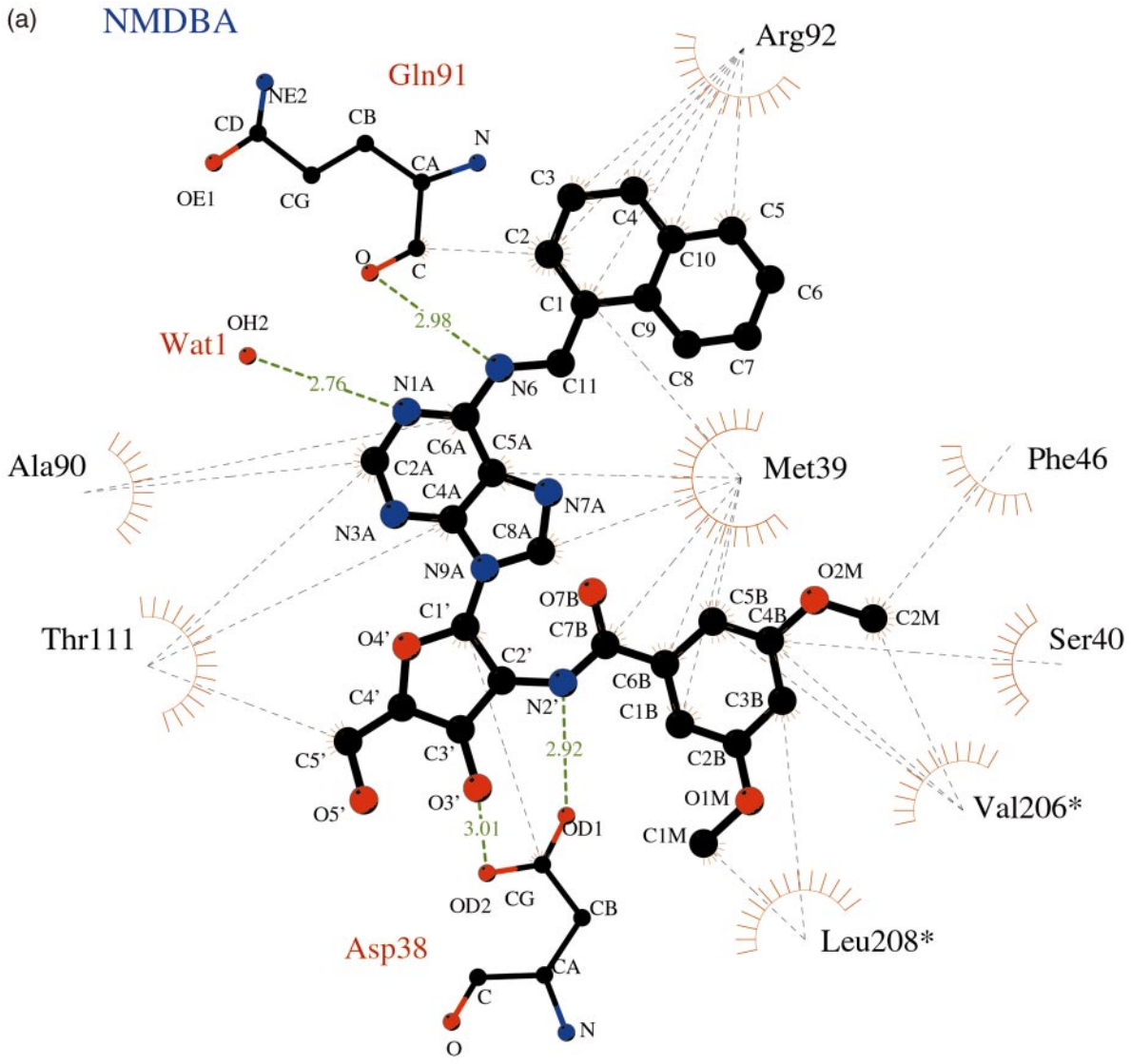


**Figure 3** (*legend opposite*)

benzamido group is inserted into a cleft between monomers, it is the local motion of residues in the middle of the polypeptide chain in response to the binding of the inhibitor that enlarge the cleft, rather than a relative motion between monomers in the GAPDH tetramer. This is evident after performing a least-squares superposition utilizing only the 358 $C^{\alpha}$ atoms of a single monomer and then comparing the relative position of the atoms in the $NAD^{+}$ and NMDBA binding tetramers. It is found that the $C^{\alpha}$ position of Met39 moves by approximately 1.9 Å in the NMDB-adenosine inhibitor complex relative to the holo enzyme complex, whereas the $C^{\alpha}$ position of Val206* from the adjacent monomer, that forms the other side of the binding pocket, moves by only 0.5 Å.

Since Met39 interacts with the dimethoxybenzamido group, and with the adenine ring and the naphthylenemethyl group, concomitant with the motion of Met39, the adenine residue, the naphthyl group, and the residues that interact with them, move in concert with similar displacements. The $C^{\alpha}$ atoms of Thr111 and Leu113 on the side of the adenine residue opposite to Met39 move by 1.1 Å and 1.7 Å, respectively, whilst the $C^{\alpha}$ atom of Arg92 on the side of the naphthyl group opposite to Met39, moves by 2.5 Å (Figure 4). Thus, the insertion of the dimethoxybenzamido group of NMDBA into the selectivity cleft between the monomers, causes the displacement of Met39, and the intimate interaction of Met39 with the rest of the inhibitor propogates this motion to the other residues involved in binding the inhibitor. Therefore we have a situation where the residues in the region of the polypeptide that form the binding pocket shift considerably on binding the inhibitor,

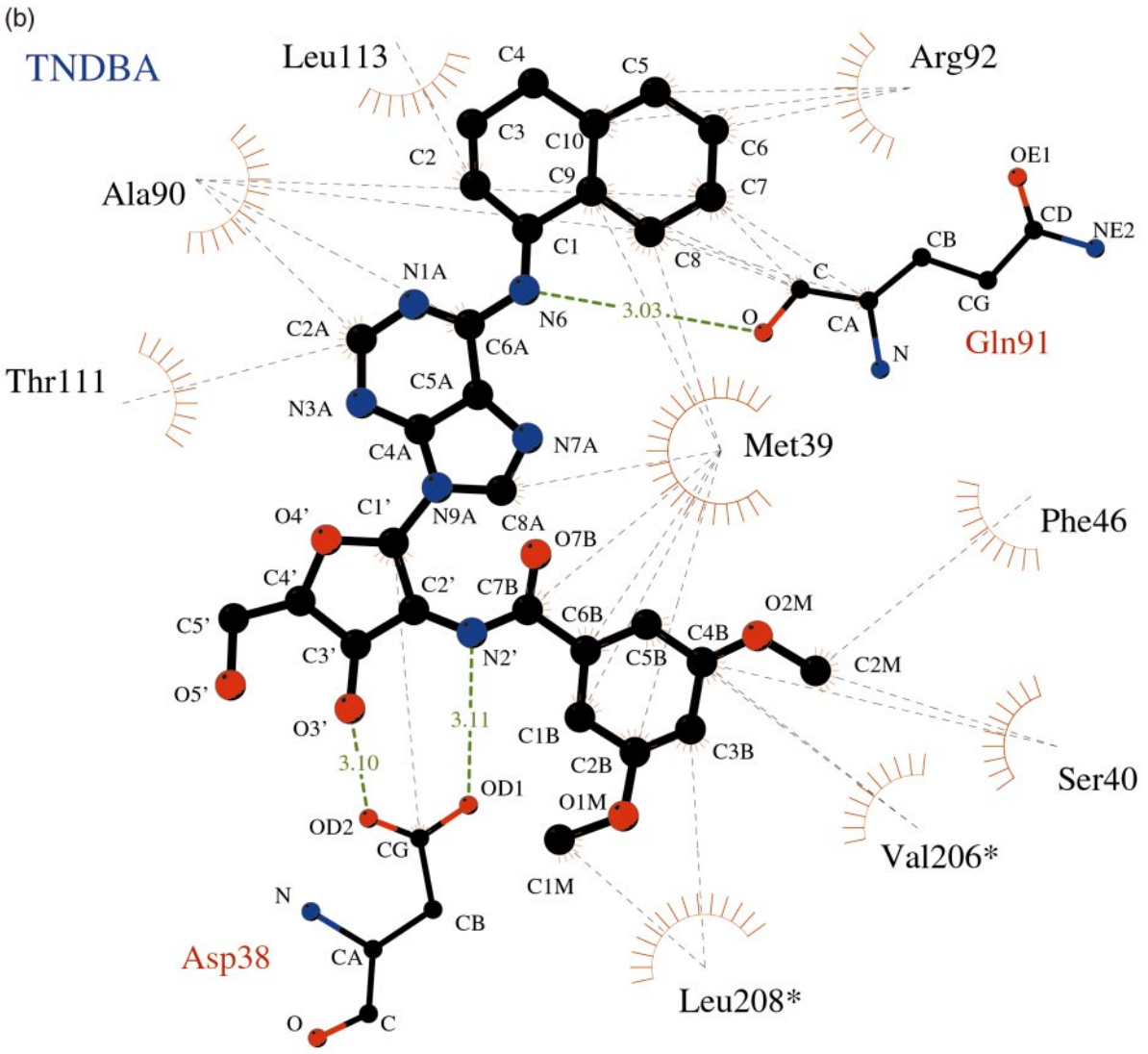


**Figure 3.** (a) Schematic drawn by LIGPLOT[42] showing interactions of NMDBA with *L. mexicana* GAPDH. (b) Schematic drawn by LIGPLOT[42] showing interactions of TNDBA with *L. mexicana* GAPDH.

whilst the inner core of the protein is relatively static.

The exquisite selectivity of these inhibitors for trypanosomatid GAPDHs as opposed to the human analogue is primarily due to the presence of the selectivity cleft in the trypanosomatid enzymes. A vital difference between human and trypanosomatid sequences at the inhibitor binding site is Pro35 in the human enzyme, instead of the equivalent Met39 of the trypanosomatids (Figure 1). In addition to playing a critical role in forming the inhibitor binding site of the trypanosomatid GAPDHs, the backbone nitrogen atom of Met39 makes a hydrogen bond to the conserved Asp38, whilst in the human enzyme, the backbone nitrogen atom of the equivalent Pro35 is unable to make a similar hydrogen bond.

## Conclusions

The elucidation of these structures of *L. mexicana* GAPDH with NMDBA and TNDBA completes a full circle of the drug design cycle,[30,31] confirming the predicted binding mode[18,22] and providing insight into the flexibility of the protein molecule. The extensive interactions of the two substituents on the adenine scaffold with the protein provide a plausible explanation for the high affinity of these adenosine derivatives for the trypanosomatid GAPDHs. The binding of these two high-affinity inhibitors is accompanied by considerable movements of the protein residues forming the binding pocket, in an example of classic induced fit. These structures of the binary complexes of designed inhibitors with *L. mexicana* GAPDH form a basis

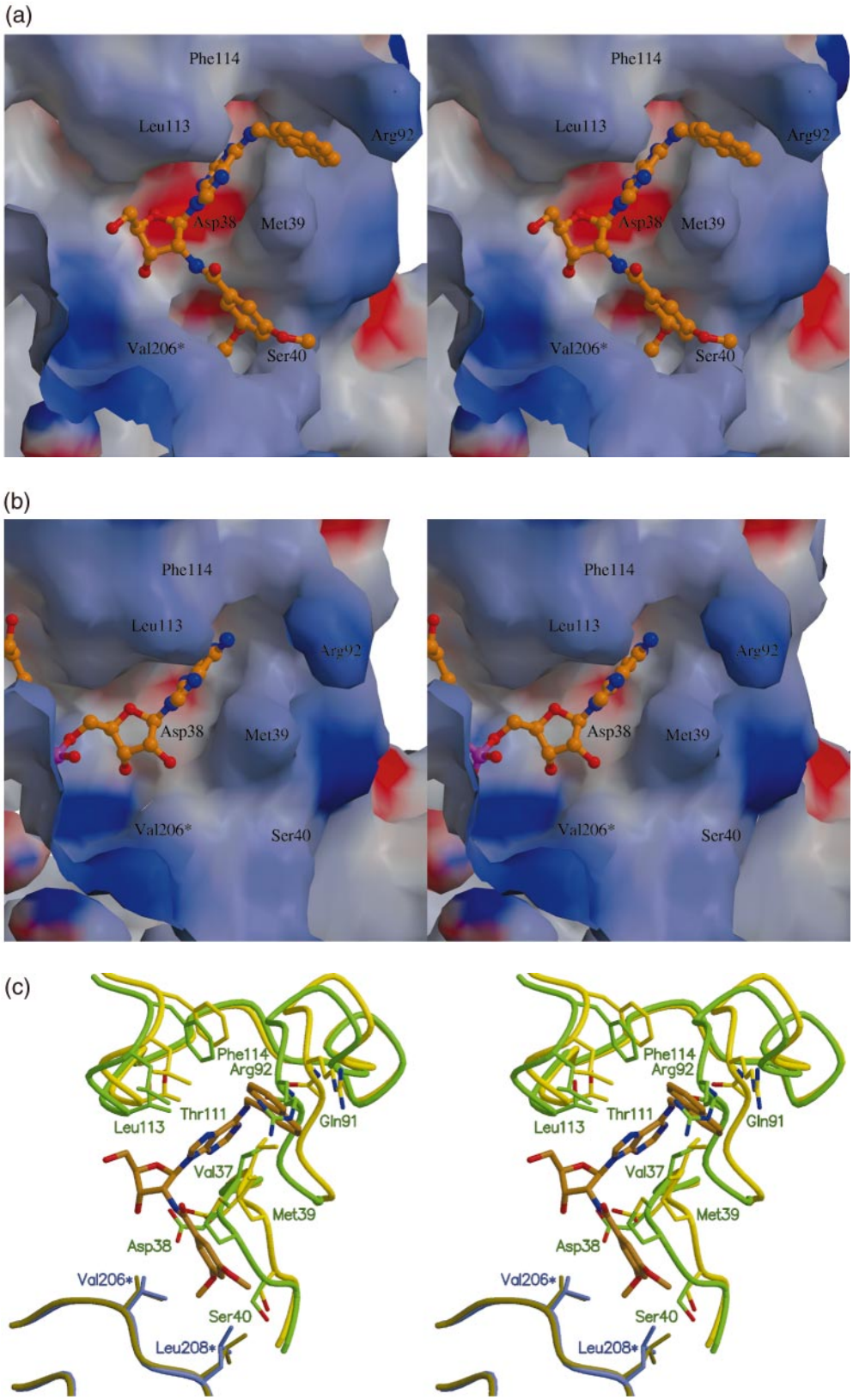


**Figure 4** (*legend opposite*)

for further development of inhibitors for all three trypanosomatid GAPDHs.

There is the possibility of mutations of Met39 generating drug-resistant versions of trypanosomatid GAPDHs. To thwart such a possibility, we are simultaneously targeting a number of glycosomal enzymes from these trypanosomatids by structure-based combinatorial chemistry methods. These include, in addition to GAPDH, the glycosomal enzymes phosphoglycerate kinase, aldolase and glycerol-3-phosphate dehydrogenase, as well as glycosomal peroxins.[32] We envision a scenario where a potent drug cocktail containing a number of inhibitors acting synergistically against these different enzymes would provide an effective treatment for the diseases caused by trypanosomatids. Such a combination of drugs that targets a number of enzymes simultaneously would be less likely to become ineffective due to drug-resistance.

The crystal structures essentially confirm the predicted binding mode of the inhibitor, although the binding site deforms considerably upon accommodating the inhibitor. The conformational changes observed in these structures open up new possibilities for the design of the next series of inhibitors. We are considering modifications on the dimethoxybenzamido group to further optimize the interactions in the selectivity pocket. This work demonstrates the power of structure-based design in the development of potent selective inhibitors.

## Materials and Methods

### Preparation of *L. mexicana* GAPDH crystals in complex with inhibitor

*Escherichia coli* expressing *L. mexicana* GAPDH were grown and lysed essentially as described.[17,33] The cell lysate was clarified by centrifugation at 10,000 ***g*** for 30 minutes, and the supernatant with the soluble protein was passed through a 0.45 μm filter. The high pI of the enzyme enabled the purification of the crude lysate by a single pass over a SPRINT (PerSeptive Biosystems) 20HS cation-exchange column, to yield apo enzyme pure enough for crystallization. The complex of *L. mexicana* GAPDH with NMDBA was prepared by mixing 500 μl of the apoprotein solution at 6 mg $ml^{-1}$ in 15 mM Hepes, 250 mM NaCl, 5 mM DTT and 1 mM PMSF with 20 μl of a 34 mM solution of the inhibitor in DMSO. The complex with TNDBA was made by mixing 520 μl of apoprotein solution with 25 μl of 22 mM TNDBA in DMSO. A large number of random and systematic crystallization screens were set up employing the sitting drop vapor diffusion method. Crystals grew under a variety of conditions, but despite the often well-defined external morphology of the crystals, they were usually mosaic and did not diffract beyond 4.0 Å. A much less regularly shape single crystal grown by mixing 2 μl of the protein-NMDBA complex with 3 μl of 5 mM DTT and 2 μl of the reservoir solution composed of 28 % (w/v) PEG1000 and 100 mM TEA (pH 7.25), diffracted to 2.5 Å and was utilized for structure determination. The crystals in complex with TNDBA were grown under similar conditions, by mixing 3 μl of protein-TNDBA complex with 3 μl of 5 mM DTT and 3 μl of reservoir solution, and they diffracted to 3.0 Å. It was interesting to note that, whilst the diffracting crystals had ill-defined external morphology, the crystals that appeared promising under the optical microscope invariably proved to be poor diffractors.

### Data collection and structure determination

Crystals of the complexes of *L. mexicana* GAPDH with NMDBA and TNDBA were each frozen in a nitrogen stream. Complete data sets were collected using X-rays with a wave-length of 1.0 Å on beam-line 5.0.2 at the Advanced Light Source, Berkeley on an ADSC CCD detector. The diffraction images were indexed and the Laue group determined using the program HKL2000,[34] which was also used to process and scale the data. The space group was then established by examining the systematic absences.

The structure in complex with NMDBA was solved by molecular replacement utilizing AMoRe.[35] The GAPDH tetramer from the holo structure (PDB code 1GYP[17]) stripped of NAD was used as a search model. The six monomers (one and half tetramers) in the asymmetric unit were then refined using CNS.[26] A difference Fourier calculated at this stage had very clear density for the inhibitor in all six copies of the GAPDH monomer in the asymmetric unit. The density was further improved by 6-fold non-crystallographic symmetry (NCS) averaging using the RAVE suite of programs.[36] A number of refinement trials were conducted using a variety of NCS restraints,[26] while monitoring the crystallographic residuals of the working set and test set of reflections. The final refinement utilized a NCS restraint weight of 25 kcal $mol^{-1}$ $Å^{-2}$ (1 kcal = 4.184 kJ), and a target deviation of 5 $Å^2$ for *B*-factor restraints. NCS restraints were applied only to the protein atoms and not to the bound inhibitor, while geometric restraints were applied to both protein and inhibitor atoms. The positions of 657 water molecules were determined from difference Fourier maps and included in the refinement.

**Figure 4.** (a) GRASP[43] surface rendition of *L. mexicana* GAPDH with NMDBA bound. The surface has been color-coded according to the electrostatic potential. Red represents negatively charged and blue represents positively charged surfaces. Clearly visible is the selectivity cleft between Met39 and Val206* (from the neighboring monomer), with the dimethoxybenzamido group of NMDBA inserted into it. (b) GRASP[43] surface rendition of holoenzyme complex of *L. mexicana* GAPDH with $NAD^+$.[17] In the absence of the inhibitor, the selectivity cleft is much smaller. (c) Superposition of the holoenzyme structure of *L. mexicana* GAPDH[17] in green and violet, and the structure in complex with TNDBA in light and dark yellow. The Figure illustrates the displacements of the protein atoms at the inhibitor binding site. In particular, the movement of Met39 effects expansion of the selectivity cleft, and this motion propagates to the other atoms involved in inhibitor binding. This Figure was made with MOLSCRIPT[38] and rendered with Raster3D.[39,40]

The protein model from the NMDBA complex, after deleting the inhibitor, was used as the starting model for the refinement of the TNDBA structure. Difference Fourier maps calculated after simulated annealing[26] followed by positional refinement, revealed clear density for TNDBA in all six copies of the GAPDH monomer in the asymmetric unit. Sixfold NCS averaging was performed to improve the quality of the map, prior to fitting a model of the inhibitor. The low resolution of the TNDBA complex data did not permit the inclusion of water molecules into the model. Further positional and *B*-factor refinement was performed using NCS restraints on the protein atoms. The quality of the two structures was assessed using PROCHECK.[37]

### Protein Data Bank accession numbers

The coordinates have been submitted to the RCSB Protein Data Bank and have been assigned codes 1I32 (*L. mexicana* GAPDH complex with NMDBA) and 1I33 (*L. mexicana* GAPDH complex with TNDBA).

## Acknowledgments

We would like to thank Ethan Merritt, Francis Athappilly, Hidong Kim, Alex Aronov and Paul Michels for useful discussions at the various stages of the project, and Stewart Turley, Abhinav Kumar, Paulene Quigley and the staff at the Advanced Light Source, Lawrence Berkeley National Laboratory for assistance during data collection. We acknowledge financial support from the National Institutes of Health (grant AI 44119) and substantial instrumentation support from the Murdock Charitable Trust to the Biomolecular Structure Center.

## References

1. WHO, (1997). *Tropical Disease Research: Progress 1995-1996, Thirteenth Programme Report*. World Health Organization, Geneva.
2. WHO, (1999). *Tropical Disease Research: Progress 1997-1998, Fourteenth Programme Report*. World Health Organization, Geneva.
3. Barrett, M. P. (1999). The fall and rise of sleeping sickness. *Lancet,* **353**, 1113-1114.
4. Wang, C. C. (1995). Molecular mechanisms and therapeutic approaches to the treatment of African trypanosomiasis. *Annu. Rev. Pharmacol. Toxicol.* **35**, 93-127.
5. Bakker, B. M., Westerhoff, H. V., Opperdoes, F. R. & Michels, P. A. (2000). Metabolic control analysis of glycolysis in trypanosomes as an approach to improve selectivity and effectiveness of drugs. *Mol. Biochem. Parasitol.* **106**, 1-10.
6. Michels, P. A. M., Hannaert, V. & Bringaud, F. (2000). Metabolic aspects of glycosomes in trypanosomatidae - new data and views. *Parasitol. Today,* **16**, 482-489.
7. Opperdoes, F. R. & Borst, P. (1977). Localization of nine glycolytic enzymes in a microbody-like organelle in *Trypanosoma brucei*: the glycosome. *FEBS Letters,* **80**, 360-364.
8. Clarkson, A. B., Jr & Brohn, F. H. (1976). Trypanosomiasis: an approach to chemotherapy by the inhibition of carbohydrate catabolism. *Science,* **194**, 204-206.
9. Noble, M. E., Verlinde, C. L., Groendijk, H., Kalk, K. H., Wierenga, R. K. & Hol, W. G. (1991). Crystallographic and molecular modeling studies on trypanosomal triosephosphate isomerase: a critical assessment of the predicted and observed structures of the complex with 2-phosphoglycerate. *J. Med. Chem.* **34**, 2709-2718.
10. Verlinde, C. L., Witmans, C. J., Pijning, T., Kalk, K. H., Hol, W. G., Callens, M. & Opperdoes, F. R. (1992). Structure of the complex between trypanosomal triosephosphate isomerase and N-hydroxy-4-phosphono-butanamide: binding at the active site despite an ''open'' flexible loop conformation. *Protein Sci.* **1**, 1578-1584.
11. Bernstein, B. E., Michels, P. A. & Hol, W. G. (1997). Synergistic effects of substrate-induced conformational changes in phosphoglycerate kinase activation. *Nature,* **385**, 275-278.
12. Bressi, J. C., Choe, J., Hough, M. T., Buckner, F. S., Van Voorhis, W. C., Verlinde, C. L. M. J., Hol, W. G. J. & Gelb, M. H. (2000). Adenosine analogues as inhibitors of *Trypanosoma brucei* phosphoglycerate kinase: elucidation of a novel binding mode for a 2-amino-$N^6$-substituted adenosine derivative. *J. Med. Chem.* **43**, 4135-4150.
13. Chudzik, D. M., Michels, P. A., de Walque, S. & Hol, W. G. (2000). Structures of type 2 peroxisomal targeting signals in two trypanosomatid aldolases. *J. Mol. Biol.* **300**, 697-707.
14. Suresh, S., Turley, S., Opperdoes, F. R., Michels, P. A. & Hol, W. G. (2000). A potential target enzyme for trypanocidal drugs revealed by the crystal structure of NAD-dependent glycerol-3-phosphate dehydrogenase from *Leishmania mexicana*. *Struct. Fold. Des.* **8**, 541-552.
15. Vellieux, F. M. D., Hadju, J., Verlinde, C. L. M. J., Groendijk, H., Read, R. J., Greenough, T., Campbell, J. W., Kalk, K. H., Littlechild, J., Watson, H. C. & Hol, W. G. J. (1993). Structure of glycosomal glyceraldehyde-3-phosphate dehydrogenase from *Trypanosoma brucei* determined from Laue data. *Proc. Natl Acad. Sci. USA,* **90**, 2355-2359.
16. Verlinde, C. L., Merritt, E. A., Van den Akker, F., Kim, H., Feil, I., Delboni, L. F., Mande, S. C., Sarfaty, S., Petra, P. H. & Hol, W. G. (1994). Protein crystallography and infectious diseases. *Protein Sci.* **3**, 1670-1686.
17. Kim, H., Feil, I. K., Verlinde, C. L., Petra, P. H. & Hol, W. G. (1995). Crystal structure of glycosomal glyceraldehyde-3-phosphate dehydrogenase from *Leishmania mexicana*: implications for structure-based drug design and a new position for the inorganic phosphate binding site. *Biochemistry,* **34**, 14975-14986.
18. Aronov, A. M., Suresh, S., Buckner, F. S., Van Voorhis, W. C., Verlinde, C. L., Opperdoes, F. R., Hol, W. G. & Gelb, M. H. (1999). Structure-based design of submicromolar, biologically active inhibitors of trypanosomatid glyceraldehyde-3-phosphate dehydrogenase. *Proc. Natl Acad. Sci. USA,* **96**, 4273-4278.
19. Gao, X. G., Garza-Ramos, G., Saavedra-Lira, E., Cabrera, N., De Gomez-Puyou, M. T., Perez-Montfort, R. & Gomez-Puyou, A. (1998). Reactivation of triosephosphate isomerase from three trypanosomatids and human: effect of suramin. *Biochem. J.* **332**, 91-96.
20. Souza, D. H., Garratt, R. C., Araujo, A. P., Guimaraes, B. G., Jesus, W. D., Michels, P. A.,

Hannaert, V. & Oliva, G. (1998). *Trypanosoma cruzi* glycosomal glyceraldehyde-3-phosphate dehydrogenase: structure, catalytic mechanism and targeted inhibitor design. *FEBS Letters,* **424**, 131-135.
21. Bakker, B. M., Michels, P. A., Opperdoes, F. R. & Westerhoff, H. V. (1999). What controls glycolysis in bloodstream form *Trypanosoma brucei*? *J. Biol. Chem.* **274**, 14551-14559.
22. Verlinde, C. L., Callens, M., Van Calenbergh, S., Van Aerschot, A., Herdewijn, P., Hannaert, V., Michels, P. A., Opperdoes, F. R. & Hol, W. G. (1994). Selective inhibition of trypanosomal glyceraldehyde-3-phosphate dehydrogenase by protein structure-based design: toward new drugs for the treatment of sleeping sickness. *J. Med. Chem.* **37**, 3605-3613.
23. Van Calenbergh, S., Verlinde, C. L., Soenens, J., De Bruyn, A., Callens, M., Blaton, N. M., Peeters, O. M., Rozenski, J., Hol, W. G. & Herdewijn, P. (1995). Synthesis and structure-activity relationships of analogs of 2′-deoxy-2′-(3-methoxybenzamido)adenosine, a selective inhibitor of trypanosomal glycosomal glyceraldehyde-3-phosphate dehydrogenase. *J. Med. Chem.* **38**, 3838-3849.
24. Aronov, A. M., Verlinde, C. L., Hol, W. G. & Gelb, M. H. (1998). Selective tight binding inhibitors of trypanosomal glyceraldehyde-3- phosphate dehydrogenase via structure-based drug design. *J. Med. Chem.* **41**, 4790-4799.
25. Mercer, W. D., Winn, S. I. & Watson, H. C. (1976). Twinning in crystals of human skeletal muscle D-glyceraldehyde-3-phosphate dehydrogenase. *J. Mol. Biol.* **104**, 277-283.
26. Brünger, A. T., Adams, P. D., Clore, G. M., DeLano, W. L., Gros, P., Grosse-Kunstleve, R. W., Jiang, J. S., Kuszewski, J., Nilges, M., Pannu, N. S., Read, R. J., Rice, L. M., Simonson, T. & Warren, G. L. (1998). Crystallography & NMR system: a new software suite for macromolecular structure determination. *Acta Crystallog. sect. D,* **54**, 905-921.
27. Skarzynski, T., Moody, P. C. & Wonacott, A. J. (1987). Structure of holo-glyceraldehyde-3-phosphate dehydrogenase from *Bacillus stearothermophilus* at 1.8 Å resolution. *J. Mol. Biol.* **193**, 171-187.
28. Murthy, M. R., Garavito, R. M., Johnson, J. E. & Rossmann, M. G. (1980). Structure of lobster apo-D-glyceraldehyde-3-phosphate dehydrogenase at 3.0 Å resolution. *J. Mol. Biol.* **138**, 859-872.
29. Yun, M., Park, C. G., Kim, J. Y. & Park, H. W. (2000). Structural analysis of glyceraldehyde 3-phosphate dehydrogenase from *Escherichia coli*: direct evidence of substrate binding and cofactor-induced conformational changes. *Biochemistry,* **39**, 10702-10710.
30. Hol, W. G. J. (1986). Protein crystallogrpahy and computer graphics- towards rational drug design. *Angew. Chemie,* **25**, 767-778.
31. Verlinde, C. L. & Hol, W. G. (1994). Structure-based drug design: progress, results and challenges. *Structure,* **2**, 577-587.
32. Kumar, A., Roach, C., Hirsh, I. S., Turley, S., deWalque, S., Michels, P. A. M. & Hol, W. G. J. (2001). An unexpected extended conformation for the third TPR motif of the peroxin PEX5 from *Trypanosoma brucei*. *J. Mol. Biol.* **307**, 271-282.
33. Hannaert, V., Callens, M., Opperdoes, F. R. & Michels, P. A. (1994). Purification and characterization of the native and the recombinant *Leishmania mexicana* glycosomal glyceraldehyde-3-phosphate dehydrogenase. *Eur. J. Biochem.* **225**, 143-149.
34. Otwinowski, Z. & Minor, W. (1997). Processing of X-ray diffraction data collected in oscillation mode. *Methods Enzymol.* **276**, 307-326.
35. Navaza, J. (1994). AMoRe: an automated package for molecular replacement. *Acta Crystallog. sect. A,* **50**, 157-163.
36. Kleywegt, G. J. & Jones, T. A. (1999). Software for handling macromolecular envelopes. *Acta Crystallog. sect. D,* **55**, 941-944.
37. Laskowski, R. A., MacArthur, M. W., Moss, D. S. & Thornton, J. M. (1993). PROCHECK: a program to check the stereochemical quality of protein structures. *J. Appl. Crystallog.* **26**, 283-291.
38. Kraulis, P. J. (1991). MOLSCRIPT: a program to produce both detailed and schematic plots of protein structures. *J. Appl. Crystallog.* **24**, 946-950.
39. Merritt, E. A. & Murphy, M. E. P. (1994). Raster3D version 2.0. A program for photorealisitc molecular graphics. *Acta Crystallog. sect. D,* **50**, 869-873.
40. Merritt, E. A. & Bacon, D. J. (1997). Raster3D: photorealistic molecular graphics. *Methods Enzymol.* **277**, 505-524.
41. Esnouf, R. M. (1997). An extensively modified version of MOLSCRIPT that includes greatly enhanced coloring capabilities. *J. Mol. Graph.* **15**, 133-138.
42. Wallace, A. C., Laskowski, R. A. & Thornton, J. M. (1995). LIGPLOT: a program to generate shematic diagrams of protein-ligand interactions. *Protein Eng.* **8**, 127-134.
43. Nicholls, A., Bharadwaj, R. & Honig, B. (1993). GRASP: graphical representation and analysis of surface properties. *Biophys. J.* **64**, 166-000.

***Edited by I. A. Wilson***

*(Received 18 December 2000; received in revised form 23 February 2001; accepted 23 February 2001)*